Neuroradiology (2012) 54:1065–1077
DOI 10.1007/s00234-012-1049-1

CONTINUING EDUCATION

Focal cortical dysplasia type IIa and IIb: MRI aspects in 118 cases proven by histopathology

Nadia Colombo · Laura Tassi · Francesco Deleo · Alberto Citterio · Manuela Bramerio · Roberto Mai · Ivana Sartori · Francesco Cardinale · Giorgio Lo Russo · Roberto Spreafico

Received: 1 February 2012 / Accepted: 22 May 2012 / Published online: 14 June 2012

Abstract
Introduction This study aims to review the magnetic resonance imaging (MRI) aspects of a large series of patients with focal cortical dysplasia type II (FCD II) and attempt to identify distinctive features in the two histopathological subtypes IIa and IIb.
Methods We retrospectively reviewed the MRI scans of 118 patients with histological proven FCD IIa (n=37) or IIb (n=81) who were surgically treated for intractable epilepsy.
Results MRI was abnormal in 93 patients (79 %) and unremarkable in 25 (21 %). A dysplastic lesion was identified in 90 cases (97 %) and classified as FCD II in 83 and FCD non-II in seven cases. In three cases, the MRI diagnosis was other than FCD. There was a significant association between the presence of cortical thickening (p=0.002) and the "transmantle sign" (p<0.001) and a correct MRI diagnosis of FCD II. MRI positivity was more frequent in the patients with FCD IIb than in those with FCD IIa (91 % vs. 51 %), and the detection rate of FCD II was also better in the patients with type IIb (88 % vs. 32 %). The transmantle sign was significantly more frequent in the IIb subgroup (p=0.003).
Conclusions The rates of abnormal MRI results and correct MRI diagnoses of FCD II were significantly higher in the IIb subgroup. Although other MRI stigmata may contribute to the diagnosis, the only significant correlation was between the transmantle sign and FCD IIb.

Keywords Epilepsy · Focal cortical dysplasia type IIa and IIb · MRI imaging

N. Colombo (✉)
Department of Neuroradiology, Ospedale Cà Granda Niguarda,
Piazza Ospedale Maggiore 3,
20162, Milano, Italy
e-mail: Nadia.Colombo@OspedaleNiguarda.it

L. Tassi · R. Mai · I. Sartori · F. Cardinale · G. Lo Russo
Claudio Munari Epilepsy Surgery Center, Ospedale Niguarda,
Milano, Italy

F. Deleo · R. Spreafico
Department of Epilepsy Clinic and Experimental
Neurophysiology, IRCCS Foundation Neurological Institute
"C. Besta",
Milano, Italy

A. Citterio
Department of Neuroradiology, Ospedale Cà Granda Niguarda,
Milano, Italy

M. Bramerio
Department of Pathology, Ospedale Niguarda,
Milano, Italy

Introduction

Focal cortical dysplasia type II (FCD II) are highly epileptogenic lesions that are frequently associated with early-onset drug-resistant partial epilepsy (DRPE). They were first described by Taylor et al. in 1971 in specimens resected from epileptic patients as focal lesions characterised by severe cortical lamination disruption, the presence of dysmorphic neurons littered throughout all but the first layer of the cortex, and, in most cases, grotesque cells of uncertain origin called "balloon cells" (BCs). On the basis of the original description and most recent classification systems [1–4], two histological subgroups of FCD II are recognised: IIa characterised by the presence of dysmorphic neurons and IIb with additional BCs. Detection of these lesions during the pre-surgical workup is crucial because it affects surgical decisions and improves post-operative outcomes [5, 6].

The use of magnetic resonance imaging (MRI) allows many cases of FCD II to be visualised in vivo in epileptic

patients; however, the challenge for neuroradiologists is to recognise very small and subtle lesions that escape MRI detection. On the basis of current opinion, the most frequent MRI features of FCD II include: increased cortical thickness, blurring of the gray/white matter (GM/WM) junction on T1-weighted images (T1WI) and T2-weighted images (T2WI), an increased signal of subcortical WM on T2WI and fluid-attenuated inversion recovery(FLAIR)-T2WI, and a decreased signal on T1WI (both 3D gradient echo and inversion recovery [IR] images). The WM signal alterations frequently taper towards the ventricle delineating the so-called "transmantle sign". Abnormal cortical gyrations and sulcations (which can be better evaluated by means of 3D-volume sequences and surface rendering reconstructions) are frequently encountered, ranging from focal enlargement of the subarachnoid spaces [7] to highly dysmorphic cortical convolutions with deeply running sulci. An increased T2-signal within the affected cortex can also be found.

Many published studies have described the MRI characteristics of FCD II [1, 8–17], but none has yet systematically evaluated the presence of each individual MRI sign in a large series of patients with histologically verified FCD II in an attempt to identify differential imaging features for the two FCD II subgroups (IIa and IIb). We retrospectively reviewed the MRI characteristics of a large cohort of patients undergoing surgery for DRPE and histologically characterised having FCD IIa or FCD IIb.

Materials and methods

Patient selection

Between June 1996 and December 2010, 941 patients with DRPE underwent resective surgery at the "C. Munari" Epilepsy Surgery Centre in Milan, Italy, after extensive electroclinical and neuroimaging investigations. In order to define the epileptogenic zone (EZ: the cortical area of seizure generation and propagation), the pre-surgical evaluation included: (a) the collection of anamnestic data in order to establish the type of epilepsy, age at seizure onset, and seizure frequency; (b) a neurological examination; and (c) electroencephalography (EEG) or video-EEG (VEEG) with at least one ictal recording in order to relate EEG events to the clinical aspects of the seizures. If the electroclinical and MRI findings did not identify the EZ sufficiently precisely, the patients underwent invasive pre-surgical stereo-EEG (SEEG). No other imaging technique (SPECT, PET) was used.

One hundred and thirty-three patients (14 %) had a histopathological diagnosis of FCD II not associated with any other pathological condition. Of these, 118 subjects with comparable and good/excellent quality MRI scans were selected for retrospective study. Patients identified as having FCD type III, dual or double pathology on the basis of the most recent classification of the International League Against Epilepsy (ILAE) [4] were excluded from the analysis.

Histopathological classification

The surgical specimens were fixed in 10 % neutral buffered formalin, embedded in paraffin, and processed routinely. Serial 7-μm sections were stained with haematoxylin and eosin, thionin, Luxol Fast Blue or Bielschowsky stain, and other sections were immunostained using antibodies against glial fibrillary acid protein (GFAP, Boehringer Mannheim, Germany), neurofilaments (2F11 monoclonal, DAKO, Germany), microtubule-associated protein-2 (MAP2, Boehringer Mannheim, Germany), and neuron-specific nuclear protein (NeuN, Chemicon International, Temecula, CA). The immunoperoxidase procedure has been described in detail elsewhere [1]. Diagnosed on the basis of the criteria of Blumcke et al. [4], FCD II was defined as the presence of profound cortical layering disruption and cytological abnormalities characterised by dysmorphic neurons (FCD IIa) and balloon cells (FCD IIb).

The slides were reviewed independently by three neuropathologists, one of whom had not been involved in the initial diagnoses and was unaware of the electroclinical data, MRI findings, and surgical outcomes. Disagreements were discussed and a consensus diagnosis was reached. Of the 118 patients evaluated on the basis of these procedures, 37 were classified as having FCD IIa (31 %) and 81 as having FCD IIb (69 %).

MRI parameters

The MRI scanners changed during the study period. Nevertheless, all of the patients were scanned using a 1.5-T magnet (Philips ACS-NT & Achieva) and comparable protocols, including (at the beginning of the study period) a transverse dual-echo spin-echo (SE) sequence of the entire brain (TR=2,000/2,500 ms; TE=20-90 ms; 1 acquisition; slice thickness=5 mm; 10 % intersection gap, FOV=230 mm; matrix size=128 x 256), which was replaced by turbo-spin-echo (TSE)-T2W sequence (TR=4,400 ms, TE=100 ms: 2 acquisitions, slice thickness=5 mm, 10 % intersection gap, FOV=230 mm; matrix size=380×240, turbo factor 15) and TSE fluid-attenuated inversion recovery (FLAIR)-T2W sequence (TR=11,000 ms; TE=140 ms; TI=2,800 ms; 4 acquisitions; slice thickness=3 mm; 10 % intersection gap, FOV=230 mm, matrix size=250×212, turbo factor 53); sagittal & coronal TSE FLAIR-T2W sequences acquired using the same parameters as the axial sequence; coronal TSE-TW2 sequence (TR=3,200 ms; TE=100 ms, 3 acquisitions; slice thickness=3 mm; 10 % intersection gap; FOV=230 mm, matrix size=256x205;

turbo factor 15); and coronal TSE inversion recovery (IR)-T1W sequence (TR=2,300 ms; TE=15 ms; TI=400 ms; 2 acquisitions; slice thickness=3 mm; 20 % intersection gap; FOV=230 mm; matrix size=256×205; turbo factor 5). The total scan time was about 45 min.

All of the patients also underwent 3D-volume fast field echo (FFE) T1W imaging in the sagittal or axial plane (TR=30 ms; TE=4.6 ms; 1 acquisition; 25° flip angle, 1 mm thick contiguous slices; FOV=250 mm; matrix size=512×512), and the source images were used for multiplanar (MPR) and volume rendering (VR) reconstructions. No intravenous contrast medium was ever injected. The coronal sequences were localised over the suspected EZ indicated by the electroclinical data.

MRI evaluation

The MRI scans were retrospectively and independently reviewed by means of conventional visual analysis by two experienced neuroradiologists (NC and AC) who were involved in the epilepsy programme and were aware of the general neuropathological diagnosis of FCD II but blinded to the histopathological subgroups. In the retrospective MRI evaluation, the location of the EZ revealed by the electroclinical data was also considered. Discrepancies between the reviewers led to a combined re-evaluation of the case until a consensus was reached.

The following individual MRI aspects were considered: (1) cortical thickening; (2) GM/WM junction blurring; (3) WM hypersignal on TSE-T2WI and FLAIR-T2WI; (4) WM hyposignal on T1WI; (5) tapering of WM signal changes towards the ventricle (the transmantle sign); (6) cortex hypersignal on T2WI; and (7) gyral/sulcal anomalies. Subcortical WM hyperintensity on T2WI and hypointensity on T1WI were subjectively judged as absent or present. Increased cortical thickness and blurring of the GM/WM junction were specifically evaluated on different MRI sequences: T1W (TSE-IR and/or 3D volume FFE T1W) and T2W (TSE-T2W and FLAIR-T2W). Inside wider lesions, we also analysed the distribution of these variables and WM signal changes and classified them as focal or diffused. All of the MRI variables were selected on the basis of our radiological experience and previous published FCD II data [1, 8–17].

A specific MRI diagnosis of FCD II was made when a combination of its distinctive signs was encountered [15]. When the MRI data suggested a dysplastic lesion but some particular features of FCD II were missing, the lesion was classified as FCD non-II.

The above imaging variables were considered in the case of adults and pediatric patients aged >3 years (when myelination is largely completed). In the two children studied when they were about 1 year old, the MRI diagnosis of FCD was mainly based on the presence of gyral anomalies as the ongoing process of myelination prevented any evaluation of signal differences between GW/WM and the transmantle sign. Our series did not include any neonates or infants aged <6 months, for whom different imaging variables should be considered [9].

We determined the prevalence of each radiological sign in the two groups differentially classified by MRI as FCD II and non-II, and in the two neuropathological subgroups (IIa and IIb). The dysplastic lesions were classified as small and large on the basis of their extension using semi-quantitative criteria; the small lesions included those located deeply along or at the botton of sulci [18]. On the basis of their anatomical location, they were also classified as lobar (involving a single lobe) or multilobar when they involved at least two lobes.

Statistical analysis

Contingency table analysis was used to evaluate the relationships between the different MRI variables and the pathological subtypes of FCD (IIa or IIb). The independence of the rows and columns in the tables was evaluated using Fisher's exact test, which was also used to evaluate the relationships between the MRI variables and the specific MRI diagnosis of FCD II. If the outcome was multinomial, the residual pattern and/or the collapsing/omission of categories was used to determine the categories of the contingency table that were probably creating the lack of independence.

The Mann–Whitney test was used to compare the number of detectable radiological signs in each patient in the groups

Table 1 Patient characteristics and surgical outcomes

Histology	M/F	Age at clinical onset (years)[a]	Age at surgery (years)[a]	Seizure duration at surgery (years)[a]	No. of seizure per month[a]	Surgical outcome Engel class I[b]
FCD IIa (n=37)	22/15	0–17 (3±5)	1–53 (8±20)	1–43 (7±17)	1–600 (35±67)	25 (68)
FCD IIb (n=81)	38/43	0–30 (4±6)	1–52 (24±23)	1–46 (16±16)	0–500 (35±90)	74 (91)
Total (n=118)	60/58	0–30 (4±6)	1–53 (21±25)	1–46 (16±18)	0–600 (35±90)	99 (84)

[a] Range: the numbers in parentheses are median values±IQR

[b] Number (%) of patients free of seizures after >2 years

Table 2 Comparison of histopathology and retrospective MRI diagnosis

Histopathology	Abnormal MRI	MRI diagnosis of FCD		Normal MRI
		n=90		
		FCD II (%)	FCD non-II	
FCD IIa (*n*=37)	19 (51)[a]	12 (32)	4	18 (49)
FCD IIb (*n*=81)	74 (91)	71 (88)	3	7 (9)
Total 118	93 (79)	83 (70)	7	25 (21)

In brackets: percent of row

[a]Including three patients with a neuroradiological diagnosis other than FCD

with MRI diagnoses of FCD II and non-II. All of the analyses were made using SPSS software (version 17 for Windows). The study design, which only allowed the inclusion of patients with histologically proven FCD II, prevented any analysis of the specificity of the signs.

Results

Table 1 shows the general characteristics of the patients in the two neuropathological subgroups, including surgical outcome.

The cohort as a whole consisted of 60 males and 58 females with a median age at epilepsy onset of 4 years (IQR 6; range 0–30) and a median age at surgery of 21 years (IQR 25; range 1–53). The median time to surgery was 16 years (IQR 18, range 1–46) and the median seizures frequency per month was 35 (IQR 90, range 0–600). The surgical outcome was very favourable, with 99 patients (84 %) in Engel class I after a minimum of 2-years' clinical follow-up: 74 patients with FCD IIb (91 %) and 25 with FCD IIa (68 %).

General MRI results

Upon re-evaluation, the MRI findings were abnormal in 93 patients (79 %) and normal in 25 (21 %) (Table 2). The abnormal cases included three subjects in whom small FCDs were overlooked at the time of the pre-operative MRI evaluation. A total of 90 FCDs (76 %) were detected by MRI: 83 (70 %) classified as FCD II and seven (6 %) as FCD non-II (Table 2). The latter group included two cases with very subtle MRI alterations consisting of areas of gyral anomalies, with an apparently thickened cortex, mild blurring of the GM/WM junction, and a slightly increased signal in T2WI of the subcortical WM, but without a transmantle sign, and diffuse cortical atrophy in one case. The remaining five patients all had one small temporal pole, with volume loss of the subcortical WM giving a moderately increased signal on T2WI and a decreased signal on T1WI; in all of these temporal lobes, a very small FCD II limited to one temporal gyrus was found at surgery.

Although the awareness that all of the 93 MRI-detected lesions were neuropathological proved FCD II, we retrospectively confirmed the MRI diagnosis of a low-grade

Table 3 MRI variables in relation to histopathological findings in 90 patients with an MRI diagnosis of FCD

MRI diagnosis of FCD	Histological diagnosis	MRI findings						
		WM hypersignal on T2WI/FLAIR-T2WI	WM hyposignal on T1WI	Tapering to the ventricle (transmantle sign)	Cortical thickening[a]	GM/WM blurring[a]	Gyrus anomalies	GM hypersignal on T2WI
FCD type II (*n*=83)	Total	80 (96)	71 (86)	76 (92)	77 (93)	76 (92)	57 (69)	17 (20)
	12 IIa	10 (83)	10 (83)	9 (75)	12 (100)	11 (97)	9 (75)	1 (8)
	71 IIb	70 (99)	61 (86)	67 (94)	65 (91)	65 (91)	48 (68)	16 (22)
FCD non-type II (*n*=7)	Total	6 (86)	5 (71)	0	3 (42)	5 (71)	3 (42)	1 (14)
	4 IIa	4	3	0	1	3	1	1
	3 IIb	2	2	0	2	2	2	0
Total (*n*=90)	Total	86 (96)	76 (84)	76 (84)	80 (89)	81 (90)	60 (67)	18 (20)
	16 IIa	14 (88)	13 (81)	9 (56)	13 (81)	14 (88)	10 (63)	2 (13)
	74 IIb	72 (93)	63 (85)	67 (91)	67 (91)	67 (91)	50 (68)	16 (22)

In brackets: percent

[a] In at least one pulse sequence

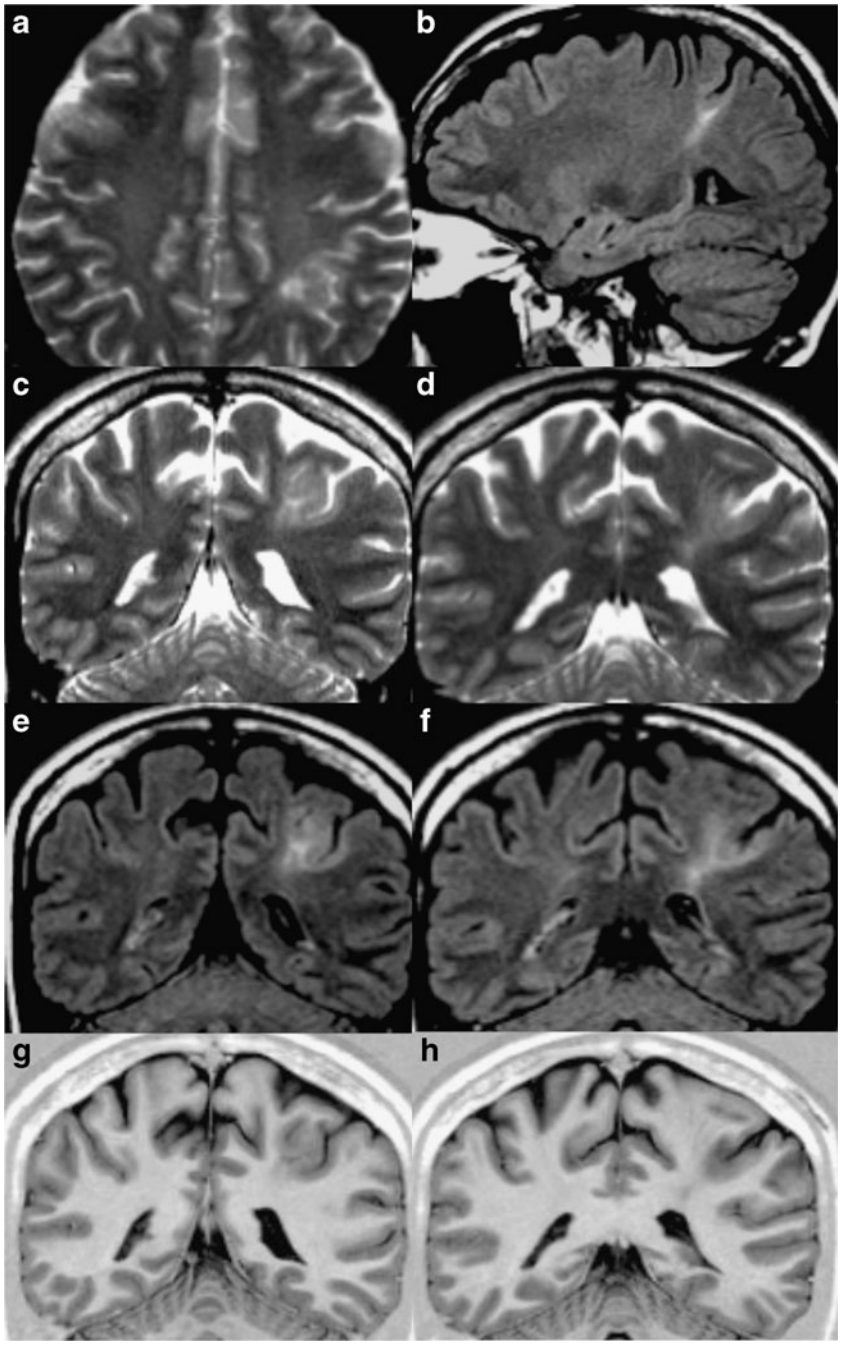

Fig. 1 FCD IIb: **a** axial TSE-T2WI, **b** sagittal FLAIR T2WI; two contiguous coronal images **c**,**d** TSE-T2W, **e**, **f** FLAIR-T2W and **g**, **h** IR-T1W. Focal thickening and abnormal convolution of the left parietal cortex which shows focal areas with blurred and other with sharp demarcation with the white matter in all pulse sequences. Increased signal on T2WI of the subcortical white matter with "funnel-shaped" extension towards the ventricle (transmantle sign) (**b**–**f**). On IR-T1WI (**h**) the transmantle sign is less evident

tumour in two patients and polymicrogyria in one. The low-grade tumours were diagnosed on the basis of the presence of very small cortical lesions apparently causing a slight enlargement of the gyrus and showing cortical/subcortical signal alterations without a transmantle sign. The case of polymicrogyria was suspected because of the presence of a focal area of multigyral cortex without cortical/subcortical signal alterations.

The correct diagnosis of FCD II was therefore made in 89 % of the patients (83/93) with abnormal MRI findings, and in 92 % of those (83/90) with an MRI diagnosis of FCD.

MRI results versus histological subgroups

FCD IIa In this subgroup of 37 subjects, the MRI findings were abnormal in 19 (51 %) and normal in 18 (49 %). MRI correctly diagnosed FCD II in 12 cases (32 %). FCD non-II was found in four cases (Table 2), low-grade tumours in two, and polymicrogyria in one.

FCD IIb Among the 81 patients assigned to this subgroup on the basis of histological findings, MRI revealed a dysplastic lesion in 74 cases (91 %) and was normal in seven (9 %). The specific MRI diagnosis of FCD II was assessed in 71 cases

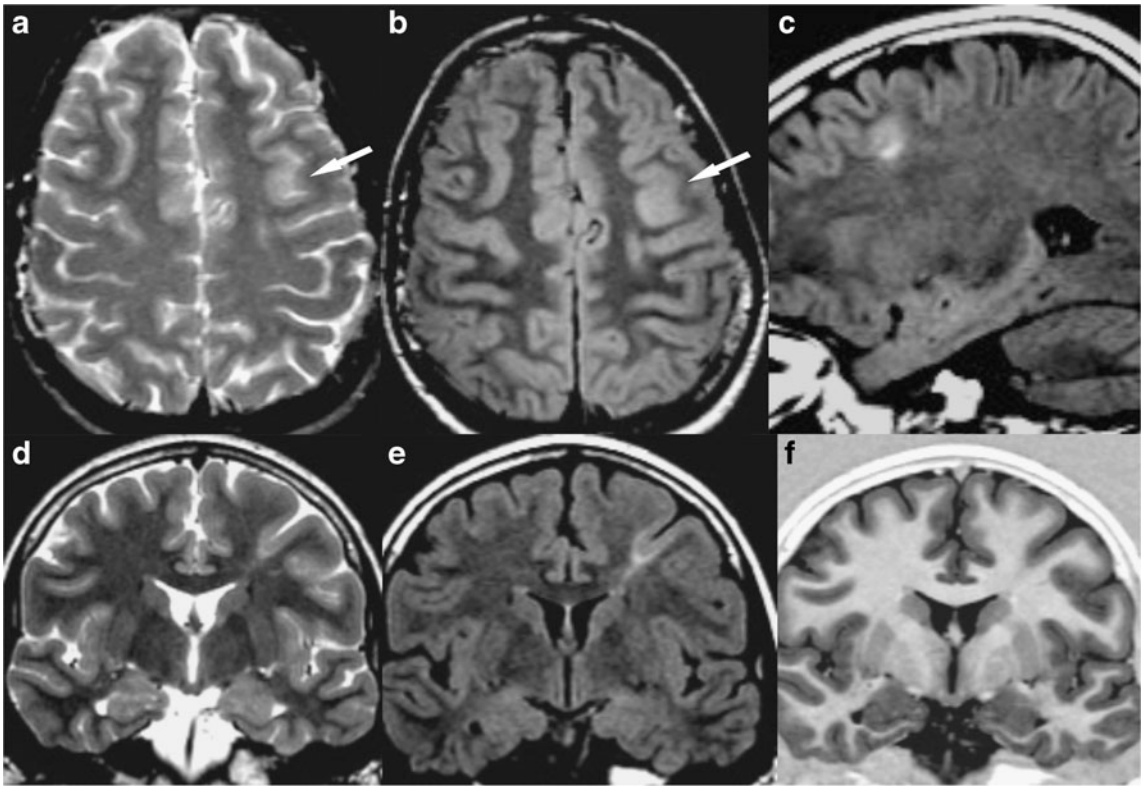

Fig. 2 FCD IIb: **a** axial TSE-T2WI, **b** axial FLAIR-T2WI; **c** sagittal FLAIR-T2WI, **d**, **e**, **f** coronal TSE-T2WI, FLAIR-T2WI and IR-T1WI. In the left frontal lobe, a very tiny dysplasia is recognized at the bottom of an abnormally deep sulcus, where the cortex appears thickened on axial images (**a**, **b**) (*white arrows*). On coronal images the transmantle sign is well seen in all pulse sequences (**d**–**f**). The GM/WM junction is blurred on axial images (**a**, **b**) and on IR-T1W coronal image (**f**), but it is sharp on coronal TSE-T2W and FLAIR-T2W images (**d**, **e**) so revealing a quite normal thickened cortex

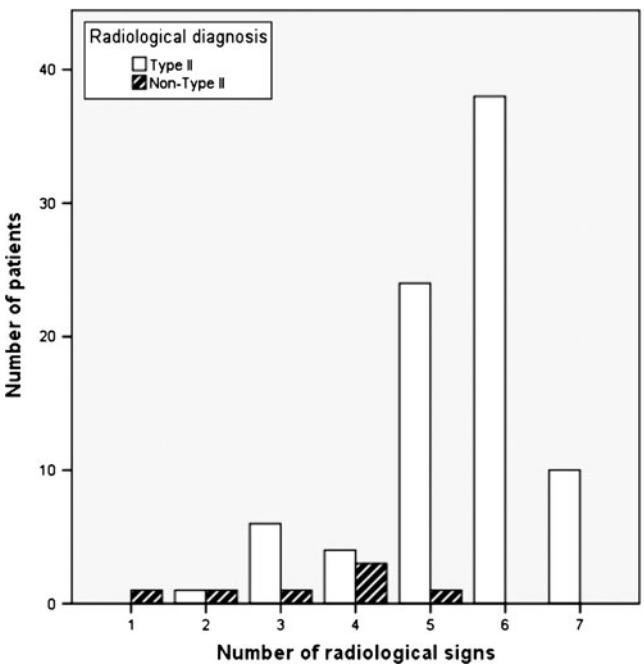

Fig. 3 Number of radiological signs correlated with number of patients with MRI diagnosis of FCD II and non-II

(88 %). In three patients, the MRI diagnosis was FCD non-II. No lesion other than FCD was reported in this group.

There was therefore a highly significant association between abnormal MRI results and the presence of BCs in the neuropathological specimens ($p<0.001$). Similarly, the detection rate of FCD II was significantly higher in the IIb histological subgroup ($p<0.001$) (Table 2).

Individual MRI signs

Table 3 shows the results of the re-evaluation of individual MRI signs in the 90 patients with an MRI diagnosis of FCD, and in the subgroups identified as FCD II (83) and as FCD non-II (7) (Figs. 1, 2, 3, 4, 5, 6, 7, and 8). In the cohort as a whole, white matter hyperintensity on T2WI was the most sensitive parameter occurring in 86 cases (96 %), but it did not assist in the differential diagnosis between FCD II and non-II (96 % vs. 86 %) (Table 3). The transmantle sign was detected 76 times as a whole (84 %), and exclusively in the cases classified as FCD II by MRI; no transmantle sign was ever observed in the patients with an MRI diagnosis of FCD non-II. Increased cortical thickness was observed in 93 % of the cases

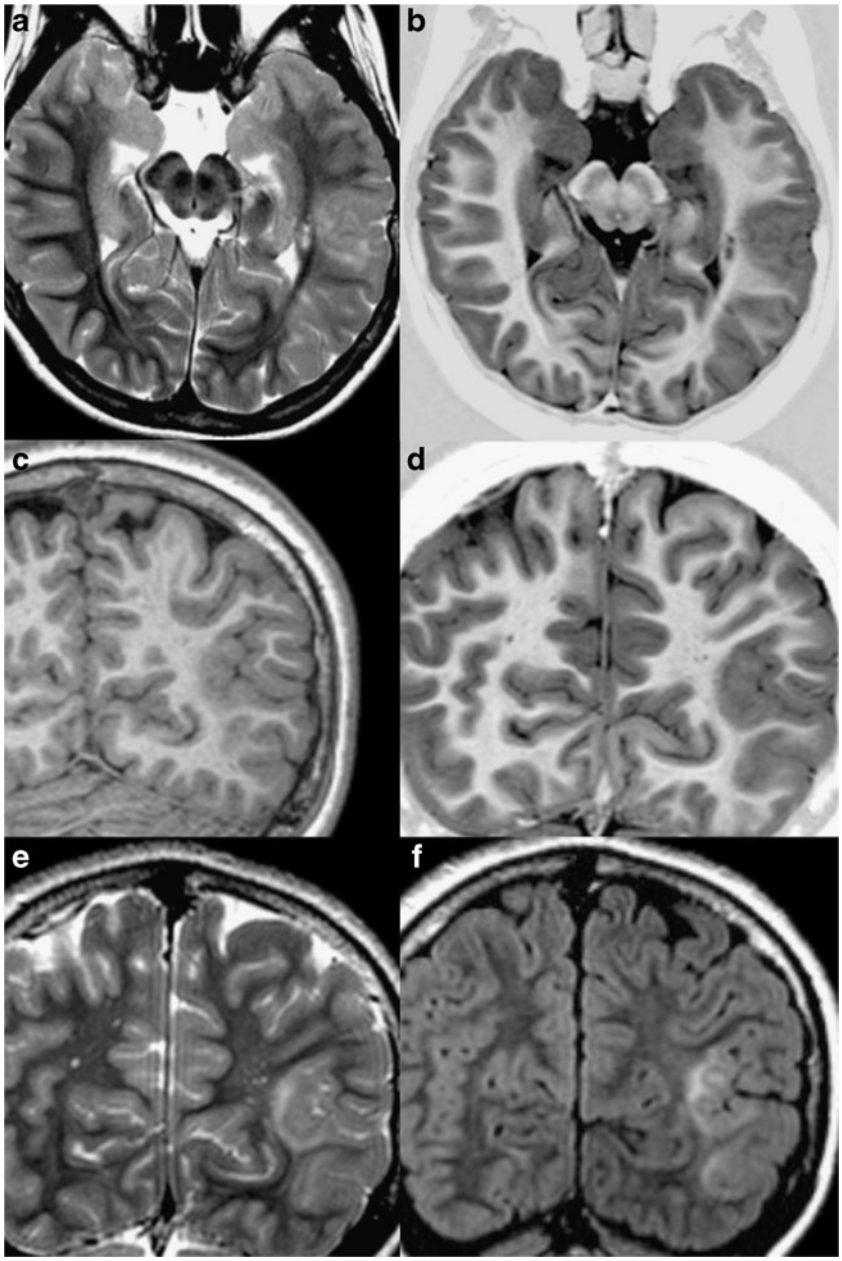

Fig. 4 FCD IIb: **a** axial TSE-T2WI, **b** axial IR-T1WI; **c** coronal 3DFFE-T1WI, **d**, **e**, **f** coronal IR-T1WI, TSE-T2WI, and FLAIR-T2WI. Abnormal gyration of the left temporo-occipital cortex which appears thickened. The GM/WM junction is blurred on T1WI (**b**–**d**) and focally blurred or sharp on TSE-T2WI and FLAIR-T2WI (**a**, **e**, **f**). No "funnel-shaped" transmantle sign is appreciated. Small perivascular spaces are present in the deep white matter lateral to the ventricle

classified as FCD II by MRI and 42 % of those classified as having FCD non-II. Consequently, the frequency of the transmantle sign and cortical thickening was significantly higher in the patients with a radiological diagnosis of FCD II ($p<0.001$ and $p=0.002$, respectively). No significant correlation was found for the other MRI signs including: GM/WM junction blurring, WM hyposignal on T1WI and abnormal gyral/sulcal pattern, although all were more frequent in the cases diagnosed as FCD II by MRI. The least frequent finding was a GM hypersignal on T2WI, which was observed in only 18 patients with an MRI diagnosis of FCD (20 %).

Clustering of the different MRI signs showed that the patients with an MRI diagnosis of FCD II were characterised by more radiological signs (mean 5.5) than those with a diagnosis of FCD non-II (mean 3.3) ($p<0.01$) (Fig. 3), thus assisting in the specific diagnosis of FCD II. With regard to the different pulse sequences acquired, the cortex was judged to be thickened in at least one in 80 patients (Table 3): in 78 on T1WI, in 63 on TSE-T2WI, and in 72 on FLAIR-T2WI (Table 4). Similarly, blurred GW/WM demarcation was observed in at least one sequence in 81 subjects (Table 3): in 79 on T1WI, in 53 on T2WI and in 68 on FLAIR-T2WI (Table 4). All of the cases showing increased cortical thickness (63) and a blurred GM/WM junction (53) on T2WI also showed the same features on T1WI and FLAIR-T2WI. It is worth noting that there were cases without blurring, but a fairly sharp GM/WM junction, which were more frequently detected on T2WI than other sequences (Figs. 2 and 4).

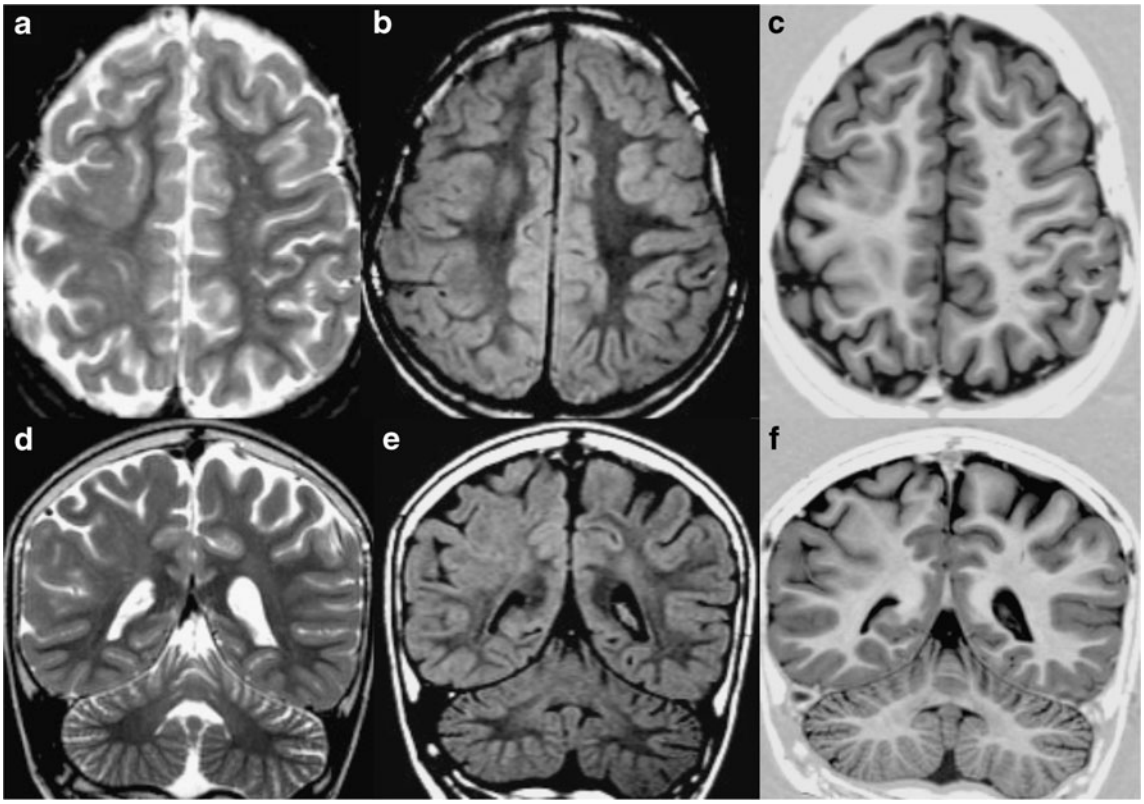

Fig. 5 FCD IIa: **a**, **b**, **c** axial TSE-T2WI, FLAIR-T2WI and IR-T1WI, **d**, **e**, **f** coronal TSE-T2WI, FLAIR-T2WI, and IR-T1WI. In the right fronto-parietal region, the cortex appears thickened, with abnormal gyration and blurred demarcation with the white matter, both on T1W and T2W images. Diffused and mild increased signal on T2WI (**a**, **b**, **d**, **e**) and decreased signal on T1WI (**c**, **f**) is seen in the subcortical white matter but no "funnel-shaped" transmantle sign is recognizable

Individual MRI signs in the histological subgroups

The prevalence of each individual MRI sign in the two neuropathological subgroups can also be derived from Table 3. The transmantle sign was significantly more frequent in patients with FCD IIb than in those with FCD IIa (p=0.003) (Figs. 1, 2, 5, 6, 7, and 8). However, it should be emphasised that the transmantle sign (defined as funnel-shaped signal alterations in the subcortical WM extending towards the ventricle) was mainly encountered in those with FCD IIb and in only two with FCD IIa (Fig. 7); in the seven remaining cases of FCD IIa, more diffuse and subtle signal alterations were detected in the subcortical and deep WM (Figs. 5, 6, and 8). There were no significant differences in the other MRI variables.

Location

Fifty-eight of the MRI-identified FCDs were small (64.5 %) and 32 were large (35.5 %). The small FCDs were unilobar in 47 cases and multilobar in 11; the large FCDs were unilobar or multilobar in 16 cases each. Sixteen of the small lesions were located at the bottom (Fig. 2) and two related to the wall of an abnormally deep and/or dysmorphic sulcus. Overall, the FCDs were more frequently located in the frontal lobe: 49/63 unilobar lesions (78 %) involved the frontal lobes and 8/27 multilobar lesions included the frontal lobe. At neuropathology, 89 % of the small and 72 % of the large lesions were FCD IIb.

Discussion

The term "focal cortical dysplasia" was coined by Taylor et al. [4, 19] to describe a peculiar malformation of cortical development that is now known and classified as FCD II. Since then however, the same term has been extensively used to describe various neuropathological variants of cortical laminar disruption. Over the last 10 years, a number of FCD classification systems based on imaging, clinical presentation, and histopathological aspects have been proposed [1–4], all of which recognise the FCD originally described by Taylor as a well-defined entity and keep it separate from the other forms. FCD II is divided into two subgroups on the basis of the absence (IIa) or presence of BCs (IIb). The differences between these two neuropathological subgroups remain to be clarified in biological, clinical, and imaging terms. Although the MRI aspects of FCD II have been extensively described in the literature, only a few studies have specifically investigated the possibly distinctive MRI features of the two subgroups [15].

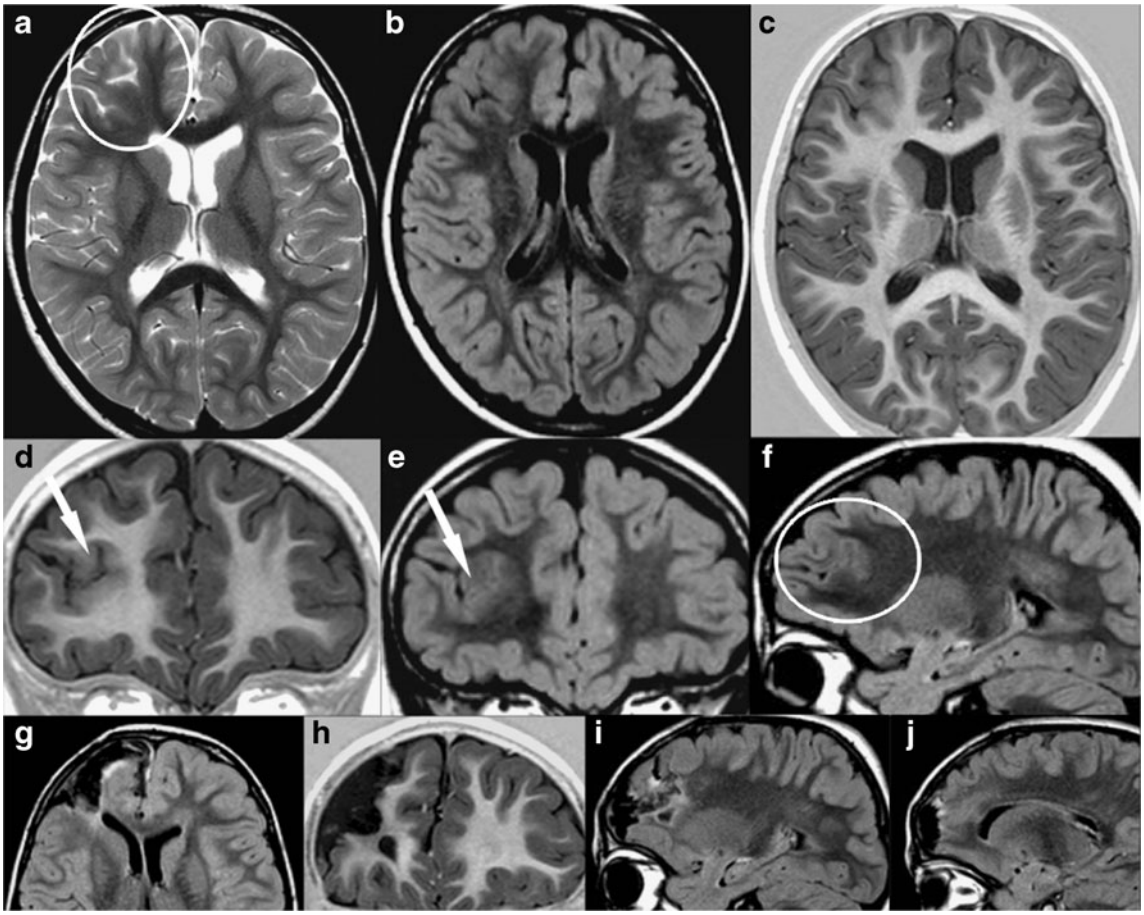

Fig. 6 FCD IIa: **a**, **b**, **c** axial TSE-T2WI, FLAIR-T2WI and IR-T1WI, **d**, **e** coronal IR-T1WI and FLAIR-T2WI, **f** sagittal FLAIR-T2WI. Post-surgical MRI: **g** axial FLAIR-T2WI, **h** coronal IR-T1WI, **i**, **j** sagittal FLAIR-T2WI. The dysplasia involving the right frontal cortex is revealed by the presence of gyration anomaly characterized by deeply running sulci (*white arrows*) with GM/WM blurring, cortical thickening, and mild-diffuse hypersignal on T2WI of the subcortical WM extending throughout the cortical mantle (*white circles*). No "funnel-shaped" transmantle sign is present

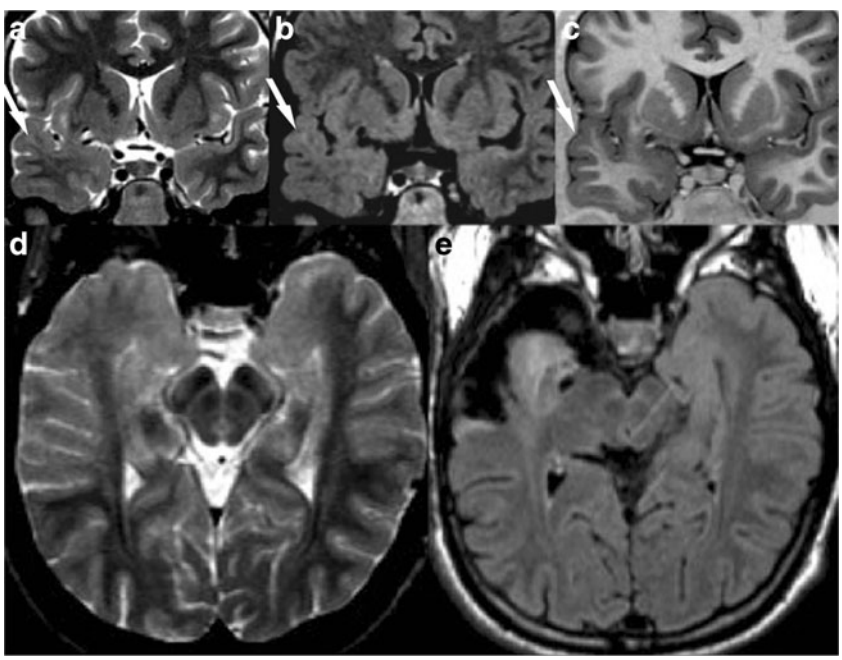

Fig. 7 FCD type IIa: **a**, **b**, **c** coronal TSE-T2WI, FLAIR-T2WI and IR-T1WI, **d** axial TSE-T2WI, **e** post-surgical MRI axial FLAIR-T2WI. On coronal images, a tiny FCD is recognizable within the first temporal gyrus on the right, mainly revealed by signal alterations of the subcortical WM with a funnel-shaped appearance (*white arrows*). Axial T2WI (**d**) show a more diffuse WM signal changes in the right temporal pole

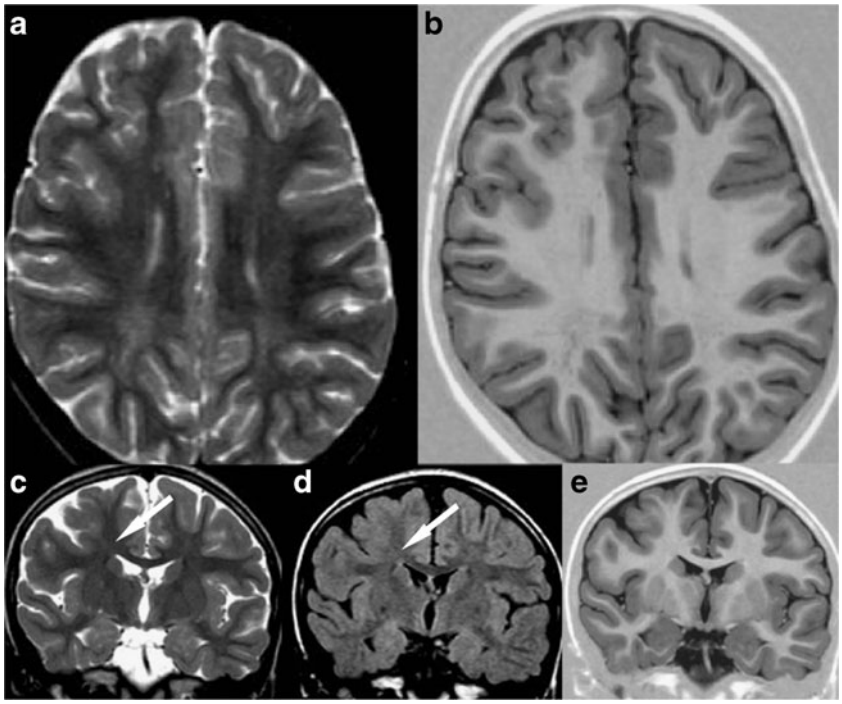

Fig. 8 FCD IIa: **a** axial TSE-T2WI, **b** axial IR-T1WI, **c**, **d**, **e** coronal TSE-T2WI, FLAIR-T2WI, and IR-T1WI. A gyration anomaly is seen in the right frontal region characterized by dysmorphic and deep sulci which are surrounded by thickened cortex. The GM/WM junction is blurred in all pulse sequences. Only mild hypersignal of the subcortical WM is seen, extending deeply, without a "funnel-shaped" appearance

We studied what is so far the largest series of histologically verified FCD II lesions with the aim of retrospectively evaluating the prevalence of various MRI signs in different sequences that can assist in the diagnosis of FCD II in order to determine whether the two subgroups are characterised by differential imaging findings. Conventional visual analysis (CVA) correctly identified 70 % of FCD II lesions in the series as a whole: 83/93 (89 %) in the group with abnormal MRI findings and 83/90 (92 %) in the group with an MRI diagnosis of FCD. It detected FCD IIb significantly better than FCD IIa lesions (88 % vs. 32 %), in line with the findings of a recently published study [20].

The diagnosis of FCD II was greatly facilitated by the presence of combinations of radiological signs. Our results confirmed that WM hyperintensity in T2WI is the most sensitive parameter, but it does not assist in the differential diagnosis of FCD II and non-II [15], and was equally present in the patients with IIa and IIb. The tapering of WM signal alterations towards the ventricle (the transmantle sign) was significantly more frequent in the cases correctly identified by MRI as FCD II ($p<0.001$) and, as previously reported in the literature [15], was significantly more frequent in patients with FCD IIb than in those with FCD IIa. However, one interesting observation was that the pattern of extension toward the ventricle was quite different in the two subgroups: it was more diffuse and less evident in the latter, whereas the "funnel-shaped" appearance described in the literature was mainly found in the former. A recent systematic analysis of the different histopathological features of FCD variants found that the "transmantle sign is a unique finding in FCD type IIb" and that it is due to a lack of myelination in the WM whose shape resembles the MRI sign [21].

Table 4 Cortical thickness and GM/WM junction pattern as evaluated in different sequences recorded in 90 patients with an MRI diagnosis of FCD

MRI signs	MRI diagnosis					
	FCD II (n=83)		FCD non-II (n=7)		Total	
Cortical thickness	>	Normal	>	Normal	>	Normal
T1WI	75	8	3	4	78	12
TSE-T2WI	60	23	3	4	63	27
FLAIR-T2WI	69	14	3	4	72	18
Blurred GM/WM junction	Yes	No[a]	Yes	No[a]	Yes	No[a]
T1WI	74	9	5	2	79	11
TSE-T2WI	48	35	5	2	53	37
FLAIR-T2WI	63	20	5	2	68	22

[a]No: sharp GM/WM demarcation

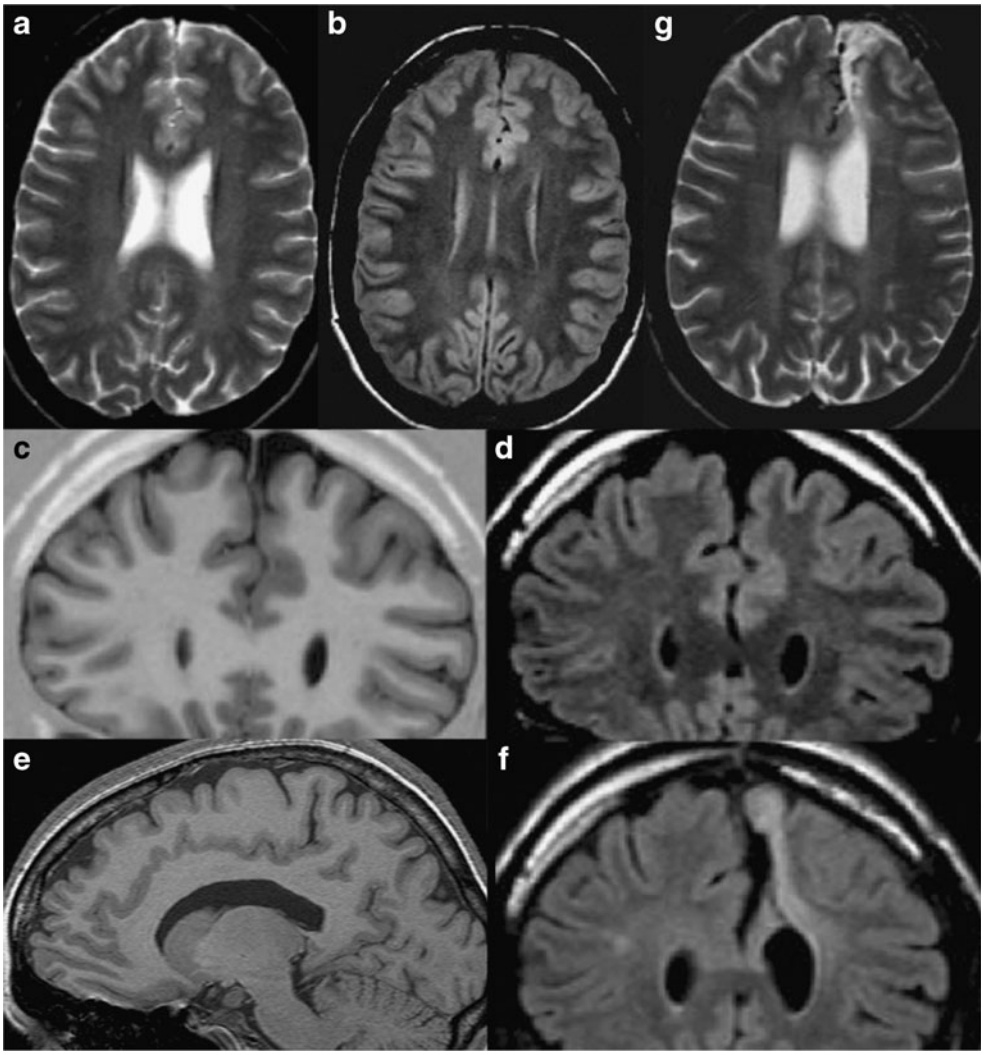

Fig. 9 Normal MRI in a patients with left frontal epilepsy: **a**, **b** axial TSE-T2WI and FLAIR-T2WI, **c** coronal IR-T1WI, **d** coronal FLAIR-T2WI, **e** sagittal 3D FFE-T1WI. Post-surgical MRI: coronal FLAIR-T2WI (**f**) and axial T2W (**g**). In the left frontal parasagittal region, no morphological or signal alterations are detectable. Based on SEEG, surgery was performed and a FCD IIa was found at neuropathology

The absence of this sign in some MRI-detected FCDs can be explained by the fact that visualising any MRI sign (particularly the transmantle sign) largely depends on an optimised angle of study, and so any sign can be missed if only pre-selected orthogonal planes are used. 3D MRI sequences with a thin partitions size can reduce this limitation by allowing multiplanar reconstructions (MPRs) and the imaging analysis of oblique planes. However, the poor GM/WM contrast intrinsic to 3D TSE-T2W and FLAIR-T2W sequences (at least in our institution) may limit their diagnostic value. Cortical thickening was also significantly more frequent in the cases correctly diagnosed as FCD II (p=0.002), but there was no significant difference between the two neuropathological subgroups IIa and IIb.

The other MRI signs of GM/WM blurring, WM hyposignal on T1WI and gyral anomalies were all more frequent in the cases diagnosed as FCD II, and also more frequent in type IIb than in type IIa; however, the differences between the two subgroups were not significant. Unlike previous studies [14, 15], we observed only a few cases of GM hypersignals on T2WI.

Cortical thickness is an important hallmark for the diagnosis of FCD, but is difficult to assess microscopically and by means of MRI analysis. Some authors have recently reported a significant increase in cortical thickness in both subtypes of FCD II on the basis of microscopic measurements of cortical regions cut perpendicularly to the pial surface [21]. The visual assessment by MRI of real cortical thickness is limited on 2D-rectilinear images because of the highly convoluted three-dimensional pattern of normal human cortex, and this may create the impression of cortical thickening if the plane of a section is oblique to the gyrus.

Furthermore, estimates of cortical thickness can be affected by the MRI pulse sequences and acquisition parameters influencing the GM/WM contrast [22]. In the case of FCD, this estimate is even more limited by the frequently abnormal convolution of the dysplastic cortex and the blurred demarcation of GM/WM junction. The latter sign has been described as one of most particular radiological markers of FCD, and more

frequent and pronounced in FCD II [1, 8, 9, 16]. However, our results confirm accumulating findings that the demarcation of GM and WM may be blurred in some cases and sharply defined in others. This difference is probably related to the degree of myelination of subcortical WM and the pulse sequences used.

Our findings indicate that T2W sequences acquired using thin sections allow the clearest delineation of the pattern of the GM/WM junction, thus facilitating the evaluation of cortical thickness. Furthermore, T2W sequences are the most suitable for this evaluation at any age, particulary in neonates and infants aged <6 months in whom dysplastic cortex is clearly revealed by the hyperintensity of unmyelinated WM. Three-dimensional (3D) MR images with a thin partition size partially overcome the limitations of 2D conventional images by allowing the use of MPR. However, the inherent complexity of cortical convolution patterns limits the identification of very small FCD lesions when only conventional rectilinear slices are analysed.

All of these limitations emphasise the need for a careful redefinition of the terminology used in imaging descriptions of FCD [17]; in cases with a blurred GM/WM junction and apparently thickened cortex on conventional MRI, our suggestion is to report "pseudo-thickening", unlike in cases with a sharply defined GM/WM junction and seemingly normal cortical thickness. In addition, we observed differences in the distribution of some MRI signs (cortical thickening, GM/WM blurring and WM signal alterations) inside the larger lesions, because they sometimes involved the entire lesion and sometimes had a focal distribution. We believe that this different behaviour may again be related to the complex geometry of wider dysplasias, which are better evaluated on T2W sequences.

The MRI findings were normal in 21 % of our study population (49 % of the patients with IIa lesions and 9 % with IIb lesions) (Fig. 9). In these cases, the lesions were probably overlooked because of their small size, their location at the bottom of a sulcus [18], and the possible limitations of our use of a 1.5-T magnet. However, it is necessary to point out that that some authors [20] have recently compared the detection rate of FCD II using morphometric and CVA at 1.5 and 3 T, and found that by means of CVA alone the rate was higher at 1.5 T. The lower field strength therefore does not seem to be a real limitation in clinical practice.

Over the last 10 years, many studies have demonstrated the advantage of MRI post-processing methods over CVA alone in identifying cortical dysplasia, and their useful utilisation in conventional MRI-normal cases [18, 22–27]. However, many post-processing techniques are time-consuming, and they are not available in all institutions.

All of the MRI-normal patients in our study had surgery planned on the basis of the electroclinical data derived from stereo-electroencephalography (SEEG). No other imaging modalities were used, including ictal/interictal SPECT or FDG-PET which are known to be helpful in localising anatomical lesions in MRI-normal patients [28] and improving surgical outcomes [29, 30]. In line with previous studies, we found a trend towards a better surgical outcome in our FCD IIb patients than in those with FCD IIa (91 % vs. 68 %) [15, 20], which may be partially explained by the more focal pattern of FCD IIb.

Conclusions

By CVA, we retrospectively evaluated the MRI scans of the largest reported series of patients undergoing surgery for DRPE with a histopathological diagnosis of FCD II (IIa and IIb). The results provide useful information for the pre-operative radiological diagnosis of this kind of lesion in clinical practice using only conventional MRI, as well as a tentative differential diagnosis of the two histopathological subgroups. Many MRI post-processing methods may offer a higher diagnostic yield especially in MRI-normal patients but, unfortunately, they are not available in all institutions.

Key learning points

1 — Focal cortical dysplasia type II (FCD II) are highly epileptogenic lesions that are frequently associated with early-onset drug-resistant partial epilepsy (DRPE).
2 — According to the original description and to the most recent classification systems two histological subgroups of FCD II are recognized: IIa characterized by the presence of abnormal cortical dyslamination and dysmorphic neurons and IIb with additional BCs.
3 — The most frequent MRI features for FCD II include: increased cortical thickness, blurred gray/white matter junction on T1WI, blurred or sharp gray/white matter junction on T2WI, increased signal on T2WI and decreased signal on T1WI of the subcortical white matter and gyration anomalies. The most peculiar feature is the tapering of the WM signal alteration towards the ventricle, the so called "transmantle sign".
4 — According to the present results, a differential MRI diagnosis between the two histopathological subgroups can be attempted. Abnormal MRI results as well as the peculiar "funnel-shaped" transmantle sign are significantly more frequent in FCD IIb.
5 — The differential MRI diagnosis has a prognostic value owing to a more favourable surgical outcome in FCD IIb.

Acknowledgment We thank Dr Alessio Moscato, Medical Physics Department, Ospedale Niguarda—Milano, for his assistance in imaging editing.

Conflict of interest We declare that we have no conflict of interest.

References

1. Tassi L, Colombo N, Garbelli R et al (2002) Focal cortical dysplasia: neuropathological subtypes, EEG, neuroimaging and surgical outcome. Brain 125:1719–1732
2. Palmini A, Najm I, Avanzini G et al (2004) Terminology and classification of the cortical dysplasias. Neurology 62: S2–S8
3. Barkovich AJ, Kuzniecky RI, Jackson GD, Guerrini R, Dobyns WB (2005) A developmental and genetic classification for malformations of cortical development. Neurology 65:1873–1887
4. Blumcke I, Thom M, Aronica E et al (2011) The clinicopathologic spectrum of focal cortical dysplasias: a consensus classification proposed by an ad hoc task force of the ILAE diagnostic methods commission (1). Epilepsia 52:158–174
5. Berg AT, Vickrey BG, Langfitt JT et al (2003) The multicenter study of epilepsy surgery: recruitment and selection for surgery. Epilepsia 44(11):1425–1433
6. Bien CG, Szinay M, Wagner J, Clusmann H, Becker AJ, Urbach H (2009) Characteristics and surgical outcomes of patients with refractory magnetic resonance imaging-normal epilepsies. Arch Neurol 66(12):1491–1499
7. Bronen RA, Vives KP, Kim JH, Fulbright RK, Spencer SS, Spencer DD (1997) Focal cortical dysplasia of Taylor, balloon cell subtype: MR differentiation from low-grade tumors. AJNR Am J Neuroradiol 18:1141–1151
8. Colombo N, Tassi L, Galli C et al (2003) Focal cortical dysplasias: MR imaging, histopathologic, and clinical correlations in surgically treated patients with epilepsy. AJNR Am J Neuroradiol 24:724–733
9. Colombo N, Citterio A, Galli C et al (2003) Neuroimaging of focal cortical dysplasia: neuropathological correlations. Epileptic Disord 5(Suppl 2):S67–S72
10. Urbach H, Scheffler B, Heinrichsmeier T et al (2002) Focal cortical dysplasia of Taylor's balloon cell type: a clinicopathological entity with characteristic neuroimaging and histopathological features, and favorable postsurgical outcome. Epilepsia 43(1):33–40
11. Ruggieri PM, Najm I, Bronen R et al (2004) Neuroimaging of the cortical dysplasias. Neurology 62:S27–S29
12. Lawson JA, Birchansky S, Pacheco E et al (2005) Distinct clinicopathologic subtypes of cortical dysplasia of Taylor. Neurology 64:55–61
13. Widdess-Walsh P, Diehl B, Najm I (2006) Neuroimaging of focal cortical dysplasia. J Neuroimaging 16:185–196
14. Fauser S, Schulze-Bonhage A, Honegger J et al (2004) Focal cortical dysplasias: surgical outcome in 67 patients in relation to histological subtypes and dual pathology. Brain 127:2406–2418
15. Krsek P, Maton B, Korman B et al (2008) Different features of histopathological subtypes of pediatric focal cortical dysplasia. Ann Neurol 63:758–769
16. Krsek P, Pieper T, Karlmeier A et al (2009) Different presurgical characteristics and seizure outcomes in children with focal cortical dysplasia type I or II. Epilepsia 50:125–137
17. Colombo N, Salamon N, Raybaud C, Ozkara C, Barkovich AJ (2009) Imaging of malformations of cortical development. Epileptic Disord 11:194–205
18. Besson P, Andermann F, Dubeau F, Bernasconi A (2008) Small focal cortical dysplasia lesions are located at the bottom of a deep sulcus. Brain 131(Pt 12):3246–3255
19. Taylor DC, Falconer MA, Bruton CJ, Corsellis JA (1971) Focal dysplasia of the cerebral cortex in epilepsy. J Neurol Neurosurg Psychiatry 34:369–387
20. Wagner J, Weber B, Urbach H, Elger CE, Huppertz HJ (2011) Morphometric MRI analysis improves detection of focal cortical dysplasia type II. Brain 134(Pt 10):2844–2854
21. Muhlebner A, Coras R, Kobov K et al (2012) Neuropathologic measurements in focal cortical dysplasia: validation of the ILAE 2011 classification system and diagnostic implications for MRI. Acta Neuropathol 123:259–272
22. Han X, Jovicich J, Salat D et al (2006) Reliability of MRI-derived measurements of human cerebral cortical thickness: the effects of field strength, scanner upgrade and manufacturer. NeuroImage 32:180–194
23. Kassubek J, Huppertz HJ, Spreer J, Schulze-Bonhage A (2002) Detection and localization of focal cortical dysplasia by voxel-based 3-D MRI analysis. Epilepsia 43(6):596–602
24. Colliot O, Antel SB, Naessens VB, Bernasconi N, Bernasconi A (2006) In vivo profiling of focal cortical dysplasia on high-resolution MRI with computational models. Epilepsia 47(1):134–142
25. Haidar H, Soul JS (2006) Measurement of cortical thickness in 3D brain MRI data: validation of the Laplacian method. J Neuroimaging 16(2):146–153
26. Bastos AC, Comeau RM, Andermann F et al (1999) Diagnosis of subtle focal dysplastic lesions: curvilinear reformatting from three-dimensional magnetic resonance imaging. Ann Neurol 46(1):88–94
27. Bernasconi A, Bernasconi N, Bernhardt BC, Schrader D (2011) Advances in MRI for 'cryptogenic' epilepsies. Nat Rev Neurol 7 (2):99–108
28. Kim SK, Na DG, Byun HS et al (2000) Focal cortical dysplasia: comparison of MRI and FDG-PET. J Comput Assist Tomogr 24:296–302
29. Salamon N, Kung J, Shaw SJ et al (2008) FDG-PET/MRI coregistration improves detection of cortical dysplasia in patients with epilepsy. Neurology 71:1594–1601
30. Chassoux F, Rodrigo S, Semah F et al (2010) FDG-PET improves surgical outcome in negative MRI Taylor-type focal cortical dysplasias. Neurology 75(24):2168–2175